International Journal of Basic and Applied Sciences, 14 (5) (2025) 131-143

International Journal of Basic and Applied Sciences

Website: www.sciencepubco.com/index.php/IJBAS
https://doi.org/10.14419/3npw0a46
Research paper

Improving The Performance of Object Detection in Underwater with Advanced Deep Learning Based Noise Reduction Techniques

S. Deepa [1], A. Umamageswari [2]*, Sankari A. [3], L. Sherin Beevi [4], K. Raja [5]

[1] Assistant Professor, Department of Computer Science and Engineering, SRM Institute of Science and Technology, Ramapuram, Chennai, India,
[2] Associate Professor Department of Computer Science and Engineering, SRM Institute of Science and Technology, Ramapuram, Chennai, India,
[3] Associate Professor, Department of Electrical and Electronics Engineering, SRM Institute of Science and Technology, Ramapuram, Chennai, India,
[4] Associate Professor, Department of Computer Science and Engineering, RMD Engineering College, Kavaraipettai, Tamilnadu, India,
[5] Professor, Department of Computer Science and Engineering, SRM Institute of Science and Technology, Ramapuram, Chennai, India,
**Corresponding author E-mail: r.umaramesh@gmail.com*

Received: July 22, 2025, Accepted: August 26, 2025, Published: September 4, 2025

Abstract

In order to identify objects that could appear suspicious, this investigation suggests an extensive method that includes pre-processing, enhancement, and noise elimination from submarine images. The method integrates the strengths of SIFT (Scale-Invariant Feature Transform) for feature extraction, CLAHE (Contrast Limited Adaptive Histogram Equalization) for enhancing underwater images to accurately identify features, and DnCNN (Deep Convolutional Neural Network) for effective noise removal through dedicated training. The method incorporates edge enhancement, color correction, brightness modulation, and preparatory processing and de-noising. The purpose of these enhancements is to visually highlight suspicious objects in the underwater images. To calculate the effectiveness of the proposed method, testing has been conducted on a variety of underwater image datasets with various settings and suspicious objects. Analysis was done in contrast to current methods for pre-processing, noise reduction, and object recognition. The results were evaluated using measurable performance metrics as SSIM, MSE, and PSNR. The experiment's findings demonstrate that the combined approach outperforms the individual methods, resulting in a higher rate of detection the 71.2% in Dn-CNN and 61.1 in CLAHE, by making suspicious items appear larger and improving the overall clarity and quality of underwater images. Numerous applications in military operations, offshore technology, maritime research and rescue, aquaculture, and other domains make it an essential sensor technology.

Keywords: *Red Compensation; Dn-CNN, CLAHE; Gamma Correction; Image Sharpening; White Balancing; SIFT.*

1. Introduction

Underwater surveillance is essential today in various industries, including marine security, submerged research, and ecological monitoring. There are unique challenges with underwater pictures due to the distinctive characteristics of the waters below. Accurately detecting an object in underwater pictures is challenging due to features like light attenuation, water turbidity, and scattering. Additionally, issues like noise, poor contrast, and low visibility further reduce the usefulness of outdated image processing and object recognition methods. To address these challenges, researchers have explored numerous methods to improve the accuracy and detection of suspicious objects. Currently, deep learning based denoising methods, such as DnCNN (Deep Convolutional Neural Network), have shown significant achievement in reducing image noise. By leveraging CNN to effectively learn and eliminate intricate noise patterns, DnCNN has proven to be a powerful solution for de-noising underwater images.
Preprocessing methods that report issues like poor contrast and restricted perceptibility may knowingly enhance the eminence of images, which increases the effectiveness of object identification systems. A common preprocessing technique called CLAHE automatically balances the distribution of a picture to improve local features and lessen the impact of uneven illumination. Furthermore, other picture-enhancing techniques may be used to further improve object identification effectiveness under adverse weather conditions. These color alteration, intensity changes, and edge enhancement techniques help make suspicious things stand out from the backdrop by improving their visual characteristics and prominence.

This study introduces a comprehensive approach that integrates DnCNN with the SIFT algorithm, CLAHE, and other image improvement techniques for the initial processing, noise removal, and identification of suspicious objects in underwater images. By employing deep learning-based de-noising, brightness adjustment through CLAHE, and enhanced feature visualization, this approach effectively addresses challenges such as poor visibility, noise, and low contrast in the deep depths of the sea. This work aims to produce a practical method to improve the recognition of apprehensive substances in underwater investigation systems. This approach aims to provide a reliable solution to strengthen safety and situational responsiveness in underwater operations. Over time, the study seeks to refine the reliability and accuracy of identifying suspicious objects in challenging underwater environments, offering significant advancements for underwater surveillance systems.

Section 2 provides related evidence on the current review; Section 3 explains the proposed method; Section 4 gives the data set; and Section 5 concludes with findings and future direction, including setup of the experiment and calculation metrics. These sections provide a detailed explanation of the planned approach. The outcomes and conclusions are shown, contrasting the effectiveness of our combined approach with other approaches.

2. Related works

Importance of underwater image de-noising and doubtful object detection, several related works highlight the integration of deep neural networks and de-noising techniques with various image improvement methods such as fusion, histogram equalization, and advanced object recognition. These techniques aim to boost contrast, make pictures more visible, and improve object identification algorithm performance in challenging underwater environments. These related studies illustrate how CLAHE-based and DnCNN-based de-noising techniques, combined with advanced image enhancement methods, contribute to the discovery of suspicious substances in underwater images. Combining these techniques enhances picture quality and boosts the effectiveness of underwater item detecting systems.

An approach to object recognition and underwater image of reduced noise that blends DL techniques with Retinex image enhancement technologies. Deep learning-powered object identification is used to identify potentially difficult-to-see things after the Retinex approach has improved picture visibility. The results demonstrate enhanced item detection skills in aquatic scenes [1]. A method for underwater image denoising and object recognition is suggested, incorporating DNN training with darkness channel augmentation. The scene's data transfer map has been computed once, utilizing the dark channel for improved image visibility. DNNs are hired for object finding in improved underwater images [2]. In another study, a multiscale mixture technique for object detection and image enhancement is introduced. This approach combines object detection with object detection to improve visibility. By using multiple image patch scales, the method enhances both global and local features, thereby boosting the presentation in interesting underwater circumstances [3]. The authors present a method for enhancing underwater images and identifying objects by combining deep learning-based noise removal with histogram equalization.

A DNN is developed to reduce noise in underwater images, while histogram equalization (HE) is useful to improve contrast. The enhanced images are subsequently processed using object recognition algorithms to detect potential threats [4]. This study presents a deep learning approach that incorporates adaptive histogram equalization (AHE) for the proposed work. Deep learning-driven object recognition is used to identify potentially difficult items after AHE is applied. This approach performs better in challenges that call for the identification of submerged items [5]. Another research proposes a hybrid approach that combines noise reduction, picture enhancement, and salient object detection for images of water. The images are used for object recognition, which entails identifying suspicious objects, after they have been improved and denoised [6].

The paper suggests a system that integrates DnCNN with SURF for underwater image de-noising and uses AHE for contrast enhancement. Additionally, object identification tools are employed to detect suspicious objects. The performance of object detection shows significant improvement when compared to traditional methods [7]. DnCNN is utilized for denoising, while CLAHE enhances the contrast. This approach leads to substantial improvements in the goal [8]. DnCNN is used to reduce noise, and CLAHE enhances contrast [9]. For object identification and underwater image enhancement, the method combines DnCNN with histogram equalization. The contrast is improved through histogram correction, and DnCNN with SUFR is used to minimize noise during the extraction of features. This ensemble approach enhances the perceptibility of suspicious objects and effectively restores underwater image clarity [10] [11].

This work investigates the usage of DnCNN along with the CLAHE with the SIFT algorithm for undersea picture denoising. The goal was to train the deep CNN network, especially for undersea photos, in order to reduce noise while enhancing image quality [12] [13]. It is a method for recovering submerged images that uses noise reduction and haze removal techniques. The authors employ a dark channel before eliminating haze, and a filter known as the median adjusts for noise reduction. The appropriate algorithms are then used to detect items of suspicion based on the restored pictures [14] [15].

This article suggests a method that combines CNNs with AHE for object detection and underwater picture enhancement [16] [17]. The researchers provide a technique that combines corrections in colors with saliency recognition for item detection and picture enhancement in water. Color enhancement techniques are used to correct color aberrations in underwater images, while saliency detection methods help identify potentially suspicious objects. Techniques for detection are then used to identify the salient items that have been detected [18] [19]. The study recommends using deep learning in conjunction with the wavelet transform in order to improve and reduce noise in underwater photos. Then, using improved and denoised photos, suspicious item recognition tasks are performed [20] [21]. The authors present a method for detecting underwater objects that combines techniques for enhancing images and reducing noise. Blurring techniques, such as wavelet-based denoising, are used to reduce noise. The enhanced images are then analyzed to detect objects, including potentially hazardous ones [22] [23].

These related studies demonstrate how to enhance and denoise underwater photos in order to identify items of suspicion by utilizing object recognition algorithms in combination with haze removal, color adjustment, noise mitigation, and deep learning [24][25]. These techniques aim to increase visibility, improve pictures, and provide accurate identification of suspicious objects. Existing techniques have several shortcomings, particularly when it comes to denoising underwater images [26] [27]. These include the complexity of underwater sceneries, the absence of ground truth information, the lack of training information, and CNNs trained on static datasets' incapacity to adapt to these shifting conditions, which reduces their usefulness in real-world applications [28] [29]. Techniques such as transfer learning, data augmentation to address the tests of blurring can be employed, with CLAHE and DnCNN, to overcome these limitations.

This method proposes a novel approach for this application for noise removal and doubtful object detection, demonstrating the effectiveness of deep learning models in enhancing image clarity and object visibility in underwater environments [30]. This work focuses on advanced de-noising techniques, aiming to enhance feature visibility for better detection accuracy [31]. Emphasizing the importance of system integration for efficient detection in practical applications [32]. This method designs a robotic system for monitoring using the YOLO (You

Only Look Once) model, showcasing the power of real-time object detection and robotic automation [33]. These studies collectively contribute to the growing body of research on enhancing object detection in challenging environments like underwater and real-time systems, with an emphasis on utilizing deep learning and de-noising techniques for better accuracy and performance [34] [35].
Recent research has significantly advanced AI-based underwater object detection through innovative denoising and enhancement techniques. This work proposed a novel algorithm integrating YOLOv5-MH, enhancing underwater object detection by improving contrast and feature extraction, ensuring robustness in complex environments [36]. A work introduced a self-supervised noise removal strategy for underwater auditory camera images, preserving essential details without prior noise modeling, making it highly effective for real-time applications [37]. This work developed a U-Net-based denoising autoencoder for underwater color restoration, which significantly improves the visual quality of submerged images, aiding in clearer object detection [38]. The method presented a diffusion model-based approach for underwater object classification, leveraging advanced imaging techniques to enhance feature learning and reduce misclassification [39]. This work proposed an improved YOLOv7 model optimized for underwater target detection, incorporating better feature extraction and faster inference speed, making it suitable for defense and surveillance operations. These studies collectively address challenges such as noise, low discernibility, and real-time processing, contributing to the advancement of underwater surveillance and military applications [40].
Prior research in underwater image processing primarily focuses on enhancing image quality through advanced denoising and contrast enhancement techniques, such as DnCNN combined with CLAHE or adaptive histogram equalization, which improve visibility and prepare images for object detection. Deep learning models like YOLOv5 and YOLOv7 have been widely adopted for real-time underwater object detection, offering fast inference and reasonable accuracy in clear or moderately challenging environments. However, these YOLO-based methods often struggle with densely cluttered scenes, low contrast, and noisy conditions typical of underwater imagery due to their reliance on large annotated datasets and potential loss of fine-grained local features. In contrast, classical feature-based methods such as the SIFT algorithm, when integrated with deep learning-powered denoising and contrast enhancement, provide robust detection by capturing invariant local features that better withstand underwater variability without extensive retraining. Hybrid approaches that combine deep learning with classical techniques show promise but often face trade-offs in computational complexity and real-time applicability. Thus, our SIFT-based approach addresses the limitations of YOLO by improving robustness in dense and low-visibility underwater conditions, offering a complementary and effective alternative for suspicious object detection in complex underwater scenes.

3. Method

Figure 1 below illustrates the overall building of the proposed method. The input pictures are initially improved through the Dn-CNN method, and then they are further improved using the CLAHE technique.

3.1. Image De-noising using Dn-CNN

For image noise reduction operations, techniques for deep learning, such as Dn-CNN, are often used. Though it may be used for enhancing underwater images, detection or classification methods are also essential for detecting problematic items. Below is an overview of a proposed technique that combines Dn-CNN picture enhancement with object recognition:
Input: Image ∈ R^(X×Y) defines the input underwater image.
1) Preparation:
Normalize the image pixels to a range between 0 and 1:

$$\mathrm{Norm(Iimage)} \Rightarrow \mathrm{Inorm}\ . \tag{1}$$

2) Model:
Define Architecture () to obtain Dn-CNN
If existing, trained model weights should load:

$$\mathrm{Dn\_CNN.loadweights('pre - trainedweights.')} \tag{2}$$

3) Denoising:
Run the normalized underwater image through:

$$\mathrm{Dn\_CNN = Onorm(Inorm)} \tag{3}$$

To obtain a refined output image:

$$\mathrm{O = Rescale(Onorm)} \tag{4}$$

4) The post-production phase
Regulate the values of pixels of O back to the range:

$$\mathrm{Orescaled = Rescale(O)} \tag{5}$$

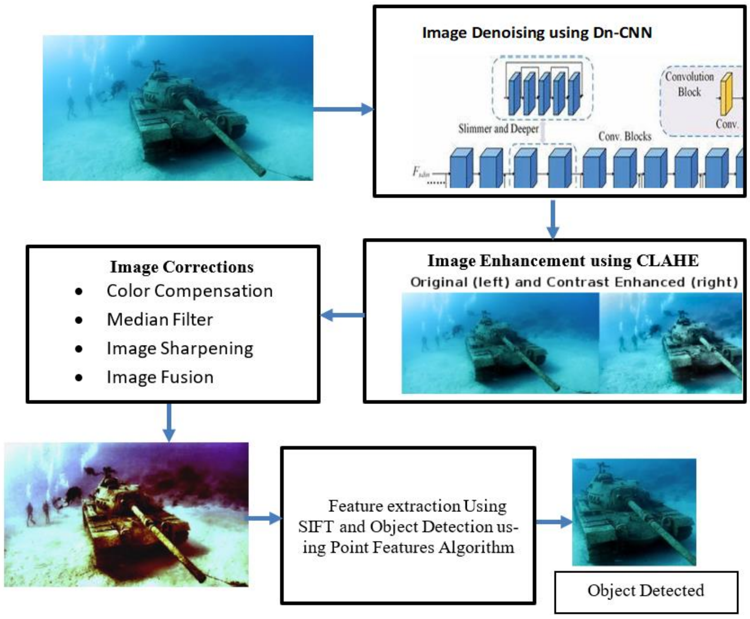

Fig. 1: Architecture of the Proposed Method.

Fig. 2: Input Image and Output Enhanced Image using Dn-CNN Algorithm.

Figure 2 (Left) The input image is shown, while the enhanced version generated using the Dn-CNN approach is displayed in Figure 1 (Right).

3.2. Image enhancement using CLAHE

The CLAHE is a widely used technique. It is particularly effective for underwater image enhancement. The method can be described as follows:
Input: Let Image ∈ RX × Yrepresent the input.
1) Preparation:
Establish the I_image pixels with values between 0 and 1: Norm (I_image) => I_norm.
2) Algorithm
Set window size as NxN
Adjust the histogram bin count: A
Length of clip: B
Split the I_image acceptable picture into NxN.
For each block: Calculate the graph H_i with B bins.
Clipping limit C with HE to H_i.
The inference from the stable histogram is to get the role of the cumulative distribution (CDF_i), which will be used to change the pixel ethics in block B_i.
Produce an output image O_norm.
3) Post-processing:
Rescale each value of the pixel Onorm to its original range: $\text{Orescaled} = \text{Rescale}(\text{Onorm})$
Rescale is a procedure that adjusts pixel ideals to the appropriate range, while Normalize() restores pixel values to a range of range between 0 to 1. Figure 3 shows the enhanced image produced by the CLAHE algorithm.


Fig. 3: CLAHE Enhanced Image.

When pre-processing information, the importance of quality filtering, information de-duplication, and privacy minimization is emphasized to prepare information for training for LLMs. The filtering method aids in the reduction of unnecessary and poor-quality information. Additionally, it lowers the computation complexity by disregarding the input's pointless pattern. The de-duplication approach eliminates duplicated samples and prevents the model's inclination toward overfitting. Lastly, privacy minimization supports the safeguarding of private information while guaranteeing information safety and compliance.

3.3. Data extraction service and data federation

Color compensation is to enhance the image's quality by correcting for color imbalances that may occur due to lighting conditions, camera settings, or other environmental factors. In this hybrid algorithm, we combine three key techniques: red compensation, white balancing, and gamma correction. The following describes the combined approach, step-by-step, with corresponding mathematical equations.
Step 1: Red Compensation
Red compensation is applied to regulate the intensity of red channels to address any overexposure or imbalance in the red channel, often caused by sensor limitations or certain lighting conditions. The red channel values are scaled by a compensation factor rcompr( ), which is determined based on the red imbalance detected in the image.
Mathematically:

$$CR'(x, y) = CR(x, y) \times rcomp \quad (6)$$

Where:
CR(x,y) - the intensity value of the red channel at pixel (x,y)
CR′(x,y) - the compensated red intensity,
rcompr is the red compensation factor (typically $0<rcomp\leq 1$)
Step 2: White Balancing
White balancing regulates the overall color balance of an image to guarantee that neutral colors (white and gray) are represented correctly. This is achieved by scaling the RGB channels based on their respective gain values derived from the average color in the image.
The white balancing correction for each color channel can be expressed as:

$$Ci'(x, y) = Ci(x, y) \times 1/\alpha i \quad (7)$$

Where:
Ci(x,y) is the intensity of the color channel iii (red, green, or blue),
Ci′(x,y) is the corrected color channel value,
αi is the white balance factor for channel iii (calculated based on the image's average color or the desired white point).
Step 3: Gamma Correction
Gamma correction compensates for the non-linear response of image sensors to light. The factor γ is used to adjust the brightness of an image. The corrected intensity values for each channel are as follows:

$$Ci'(x, y) = 255 \times (Ci'(x, y)/255)\gamma \quad (8)$$

Where:
Ci′(x,y) is the value after red compensation and white balancing for the color channel iii.
Ci′′(x,y) is the final corrected intensity value for channel iii,
γ is the gamma correction factor (typically γ=2.2 for standard correction).
Final Output: The final corrected color values CR′′′(x,y), CG′′′(x,y), and CB′′′(x,y) represent the red, green, and blue intensities of the compensated pixel at (x,y), producing a color-corrected image.
The hybrid method combines three techniques to address different aspects of color correction. Red compensation focuses on adjusting the red channel to correct any color dominance or imbalance that may have been introduced by lighting or sensor characteristics. White balancing corrects the overall image color by adjusting the gain of the red, green, and blue channels relative to one another, ensuring that neutral colors appear truly white or gray in the image. Finally, gamma correction compensates for the non-linear relationship between the pixel values and the actual light intensities in the scene, enhancing the image's brightness and contrast to match human visual perception. This combined method effectively handles color distortions caused by lighting conditions, camera sensors, and non-linear responses, ensuring more natural and visually accurate images.

Fig. 3: Color Compensated Image

3.4. ML framework and FSOBIA for predicting online buying behaviour of consumers

Image sharpening using a Laplacian filter enhances the details by emphasizing rapid intensity changes, typically at edges. The Laplacian filter is a second-order derivative filter that highlights areas with significant intensity differences, such as edges.

Step 1: Define the Laplacian Filter
The 3x3 Laplacian filter can be represented as:

$$\text{Laplacian Kernel} = \begin{matrix} 0 & -1 & 0 \\ -1 & 4 & -1 \\ 0 & -1 & 0 \end{matrix} \quad (9)$$

Alternatively, a sharpened version of the Laplacian filter (to increase edge prominence) is:

$$\text{Sharpened Laplacian Kernel} = \begin{matrix} 0 & -1 & 0 \\ -1 & 5 & -1 \\ 0 & -1 & 0 \end{matrix} \quad (10)$$

Step 2: Convolution Operation
To sharpen the image Laplacian filter is applied using convolution. For each pixel at coordinates (x, y) the sharpened value of the pixel is calculated as the weighted sum of its neighbors, weighted by the Laplacian kernel.
For RGB Channel:

$$I_{sharpened}(x, y) = I(x, y) + \alpha \cdot \sum_{i=-1}^{1} \sum_{j=-1}^{1} K(i, j) \cdot I(x + i, y + j) \quad (11)$$

Where:
I(x,y) is the intensity of the pixel at (x,y)(x, y)(x,y),
K(i,j) is the Laplacian kernel,
α is a scaling factor (typically α=1 or another chosen value for enhancing the effect).
Step 3: Apply to Color Channels
The above operation is applied to each color channel (R, G, B) of the image:

$$R_{sharpened}(x, y) = R(x, y) + \alpha \cdot \sum_{i=-1}^{1} \sum_{j=-1}^{1} K(i, j) \cdot R(x + i, y + j) \quad (12)$$

$$G_{sharpened}(x, y) = G(x, y) + \alpha \cdot \sum_{i=-1}^{1} \sum_{j=-1}^{1} K(i, j) \cdot G(x + i, y + j) \quad (13)$$

$$B_{sharpened}(x, y) = B(x, y) + \alpha \cdot \sum_{i=-1}^{1} \sum_{j=-1}^{1} K(i, j) \cdot B(x + i, y + j) \quad (14)$$

Step 4: Combine Channels
After sharpening each channel, the final sharpened image is obtained by combining the sharpened red, green, and blue channels:

$$I_{sharpened}(x, y) = [R_{sharpened}(x, y), G_{sharpened}(x, y), B_{sharpened}(x, y)] \quad (15)$$

This process enhances the edges in the image, making details more distinct.

Fig. 5: Sharpened Image.

3.5. Sift algorithm for feature extraction

The SIFT is a widely used technique in image processing for feature extraction, specifically for detecting local features in images. It is highly robust to variations in rotation, scale, and partially invariant to affine transformations, making it suitable for applications such as image stitching, object recognition, and 3D reconstruction. Below is an outline of the SIFT algorithm for feature extraction:
Step 1: Scale Space Extrema Detection
SIFT operates on a scale-space representation of the image to detect potential interest points. A scale-space is created by applying Gaussian blurring at different scales. The image $I(x, y)$ is convolved with a Gaussian kernel to generate a scale-space $L(x, y, \sigma)$, where σ represents the scale:

$$L(x, y, \sigma) = G(x, y, \sigma) * I(x, y) \quad (16)$$

Here, $G(x, y, \sigma)$ is the Gaussian function
The scale-space is built by applying different levels of Gaussian filtering with increasing σ, producing a series of images at different scales. The Difference of Gaussian (DoG) is then used to detect potential keypoints.

$$D(x, y, \sigma) = L(x, y, k\sigma) - L(x, y, \sigma) \quad (17)$$

Where k is a constant factor (usually $k=\sqrt{2}$) that determines how the scale is sampled.
Key points are identified as local extrema (minima or maxima) in both space and scale. A point (x, y, σ)It is considered an extreme if it is the minimum or maximum of the DoG compared to its neighbors in both space and scale.
Step 2: Key-point Localization
After detecting potential key points, the next step is to refine their positions. This is achieved by applying a quadratic fit to the local image structure, allowing for precise determination of the key-points' location and scale. The position of the key point (x, y, σ) is refined by using Taylor expansion to compute the 3D interpolation of the DoG function. This step involves finding the extremum of the DoG with respect to the image coordinates x,y, and scale σ. Let $D(x, y, \sigma)$ be the DoG function.
Step 3: Orientation
To ensure rotation invariance, a key point is assigned on the local image gradients in its vicinity. The gradient magnitudes $m(x, y)$ and orientations $\theta(x, y)$ are computed within a neighborhood around the key-point.
The gradient magnitude at each point (x, y) is:

$$m(x, y) = \sqrt{(\partial I(x, y)/ \partial x)^2} + \sqrt{(\partial I(x, y)/ \partial y)^2} \tag{18}$$

The orientation is given by:

$$\theta(x, y) = \operatorname{atan2}(\partial I(x, y)/ \partial y, \partial I(x, y)/ \partial x) \tag{19}$$

Step 4: Feature Matching
After extracting descriptors, SIFT features are matched between images. A nearest-neighbor search is typically used to find the best matches between keypoints in different images. A common distance measure is the Euclidean distance between two descriptors $d1$ and d2:

$$\text{distance}(d1, d2) = \| d1 - d2 \tag{20}$$

A ratio test is commonly used to eliminate ambiguous matches. It compares the distance of the closest match to the second closest match and retains only those matches where the ratio is below a specified threshold t:

$$\text{distance}(d1, d2)/\text{distance}(d1, d3) < t \tag{21}$$

Where $d1$ is the closest descriptor and $d2, d3$ are the next two closest descriptors. Typically, $t = 0.7$.
Algorithm:
- Apply Gaussian smoothing to the grayscale image Igray across multiple scales using the formula: $L(a, b, \sigma) = I\_gray(a, b) * G(a, b, \sigma)$.
- Subtract adjacent scales in the scale space pyramid to compute DoG images: $D(a, b, \sigma) = L(a, b, \sigma 2) - L(a, b, \sigma 1)$.
- Identify potential focal points or key points by locating local extrema in the DoG images across both spatial and scale dimensions.
- Use interpolation to achieve sub-pixel precision and filter out low-contrast points or edge-like features from the detected key-points.
- Calculate the dominant gradient direction in the local neighborhood of each key-point and assign it an orientation to ensure rotation invariance.
- Generate feature descriptors by extracting local image characteristics around each key-point using the SIFT descriptor.
- Compute the Haar wavelet responses for each keypoint within a rectangular region.
- Construct a feature vector using a specific layout or pattern.

To improve robustness to variations, apply additional procedures or normalize the descriptors. The extracted keypoints and their corresponding descriptors are the final result of the extraction process.

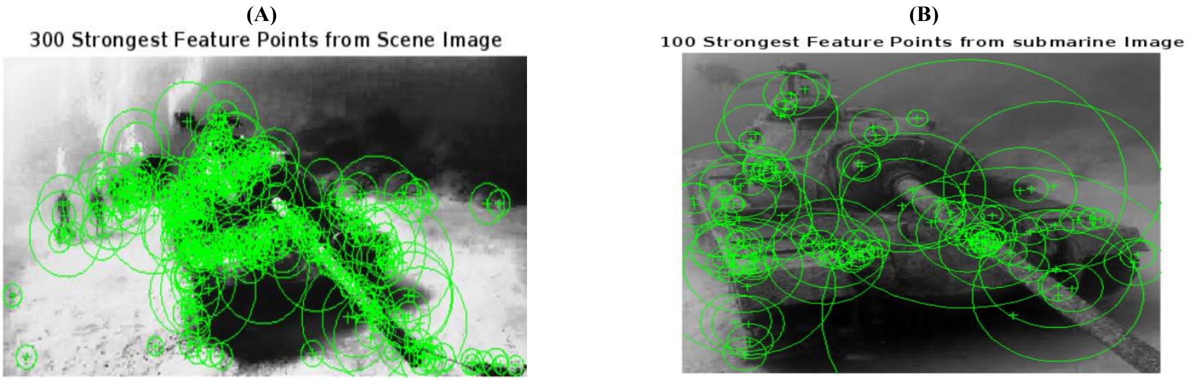

Fig. 5: (A) 300 Strong Points Extracted from the Original Image. (B) 100 Strong Feature Points Extracted from the Object to Search

Figure 6 illustrates the output of the SIFT algorithm after performing feature extraction.

3.6. Point feature matching algorithm for object detection

This process involves finding correspondences between features extracted from the input image and those from the template image. The structure of the algorithm is as follows:
Input: Image $\in R^{(X \times Y)}$ specifies the input.

1) Feature Matching:
Apply the feature extraction technique used for the reference image to the input image.
Perform the process by comparing the key-point descriptions from the input image with those from the reference image.
Use an alignment technique, such as the Randomized Sample Consensus (RANSAC) method and Nearest Neighbor Lookup, to establish correspondences between the keypoints.
2) Verification and Filtering:
Filtering techniques are applied to remove inconsistencies and enhance the quality of the outcome. The RANSAC method will be employed to reject mismatches based on the probable transformation model and predict the profile transformation between the template and input images.
Establish a threshold or use geometric approaches to evaluate whether there are enough confirmed matches for the thing to be considered detected.
3) Object Detection:
Once the connections are established and verified, the object's scene and position in the provided image can be determined. This will be achieved by applying linear transformations, such as affinal or homographic transforms, to map the points and accurately position the object in the image.
4) Output:
The ROI or boundaries indicate the location of the identified object in the input image. To handle size variations in the object, additional techniques, such as multi-scale matching and scaled spatial analysis, can be employed.

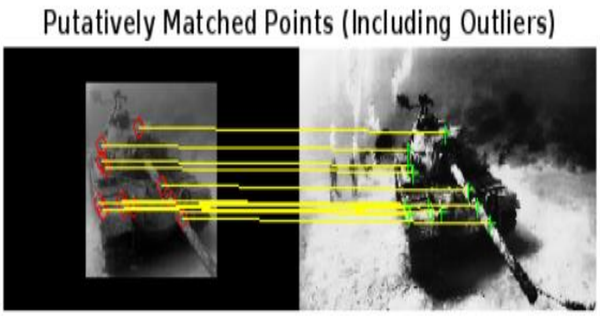

Fig. 7: Output of Feature matching- Identification of Object.

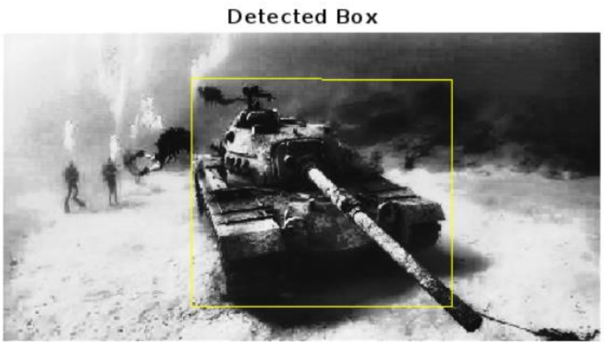

Fig. 8: Object Detection Output.

The result of the feature matching technique for identifying two objects in the image is shown in Figure 7. The suspicious objects like Torpedoes (primary offensive weapon), Missiles (some submarines launch anti-ship or land-attack missiles, e.g., cruise missiles), Naval mines, swarm drones or UUVs (in advanced military systems), and main battle tanks detected in the images are exhibited in Figure 8.

4. Results and discussions

4.1. Dataset

The Detecting Underwater Objects (DUO) dataset is designed to enhance underwater target detection by addressing challenges such as dense and blurry targets. It comprises a total of 8,893 images, separated into testing, training, and validation sets:

- Training Set: 6,671 Nos
- Testing Set: 1,111 Nos
- Validation Set: 1,111 Nos

Annotations are provided in both JSON and TXT formats, facilitating compatibility with various machine learning frameworks, including the YOLO algorithm. Regarding image dimensions, the dataset has been preprocessed to resize images to 640x640 pixels, ensuring uniformity across the dataset. Some samples are displayed in Figure 9. Additionally, the dataset includes information about lighting conditions, water depth, and the overall fineness of the captured images, including navy application-based images.

Fig. 9: Example Dataset Images

Understanding this information is crucial for comprehending the challenges posed by varying environmental conditions. The dataset includes tags or annotations that highlight the features or objects present in the images. These annotations are particularly used for tasks like object detection and classification.

The Detecting Underwater Objects (DUO) dataset comprises 8,893 images divided into training (6,671), testing (1,111), and validation (1,111) sets, all resized to 640x640 pixels for consistency with common deep learning frameworks like YOLO. It features a diverse range of object types, including marine life (fish, crustaceans), man-made objects (submerged vessels, mines, debris), and natural underwater features (coral, rocks), making it highly representative of real-world underwater scenarios, particularly naval applications. The dataset captures challenging environmental conditions such as varying turbidity levels—from clear to highly murky waters—different lighting situations, including shallow, well-lit areas and deep, dim scenes, and a range of water depths affecting color and visibility. These factors, combined with dense object clustering, motion blur, noise from suspended particles, and multi-scale object sizes, create a complex environment for object detection algorithms. Annotations are provided in both JSON and TXT formats to support various machine learning models, facilitating accurate detection and classification tasks. This rich combination of diverse objects and challenging conditions makes the DUO dataset a comprehensive resource for developing and benchmarking robust underwater detection systems.

4.2. Performance measures for de-noising

Metrics such as Mean Squared Error (MSE), Peak Signal-to-Noise Ratio (PSNR), and Structural Similarity Index Measure (SSIM) are commonly used. MSE measures the average squared difference between the original and de-noised images. Together, these metrics provide a balanced evaluation of both the fidelity and visual quality of de-noised images.

$$\mathrm{PSNR} = 10\log_{10}\frac{255^2}{\mathrm{MSE}} \tag{22}$$

$$\mathrm{MSE} = \frac{1}{M*N}\sum_{i=1}^{M}\sum_{j=1}^{N}[x(i,j) - x(i.j)]^2 \tag{23}$$

Where

MSE and PSNR are commonly utilized metrics in denoising analyses, providing a numerical evaluation of the clarity and accuracy of denoised images.

$$\mathrm{SSIM} = \frac{(2\mu_i\mu_I+Q_1)(2\sigma_{iI}+Q_2)}{(\mu_i^2+\mu_I^2+Q_1)(\sigma_i^2+\sigma_I^2+Q_2)} \tag{24}$$

The models were evaluated across a PSNR range of 36 dB to 66 dB, corresponding to noise levels between 0 dB and 20 dB. As shown in Figure 11, four levels of wavelet decomposition were performed along with soft thresholding techniques. The outcomes, presented in Table 1, highlight the performance of the proposed Dn-CNN method under varying noise power conditions. For each test, MSE and PSNR values were computed, demonstrating the model's effectiveness in suppressing noise and improving overall image quality.

Table 1 shows that an improved SSIM value indicates greater perceptual similarity between the reconstructed image and its reference, while lower MSE and higher PSNR values signify that the rebuilt image closely matches the reference in terms of texture and structure. SSIM is particularly valuable for assessing perceptual image quality as it quantifies similarity based on human visual perception. As shown in Table 1 and Figures 10, 11, and 12, the proposed approach consistently outperforms benchmark methods, achieving higher PSNR values, lower MSE, and Superior SSIM scores, thereby demonstrating enhanced denoising performance.

Table 1: PSNR, MSE, and SSIM Analysis Using Dn-CNN

Noise (dB)	PSNR	SSIM	MSE	PSNR	SSIM	MSE
	Original Image			Denoised Image		
0	55.36	0.753	0.247	60.01	0.934	0.0734
3	53.63	0.635	0.364	58.42	0.815	0.0767
5	48.32	0.462	0.628	54.47	0.754	0.325
10	42.39	0.346	0.821	47.16	0.943	0.732
15	46.28	0.416	0.741	52.65	0.771	0.525
20	50.34	0.533	0.233	58.57	0.864	0.0743

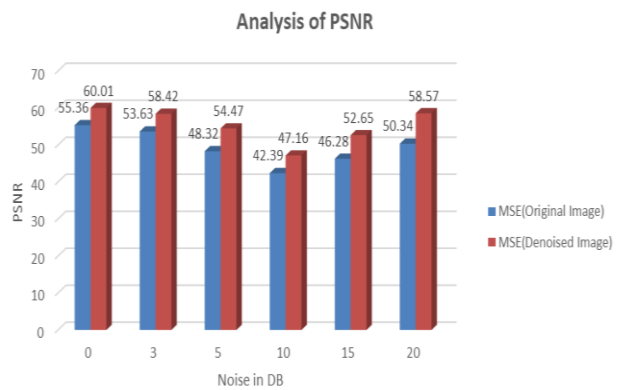

Fig. 10: Analysis of PSNR Using Dn-CNN

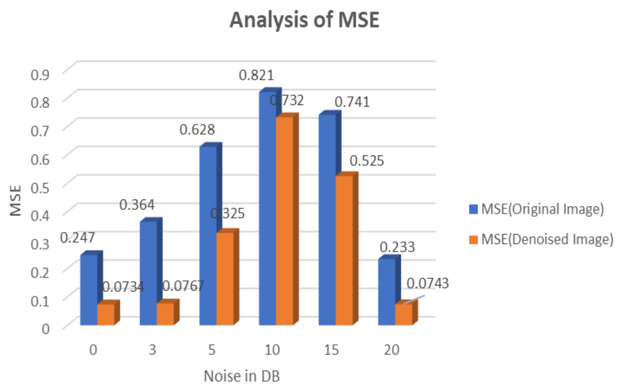

Fig. 11: Analysis of MSE Using Dn-CNN.

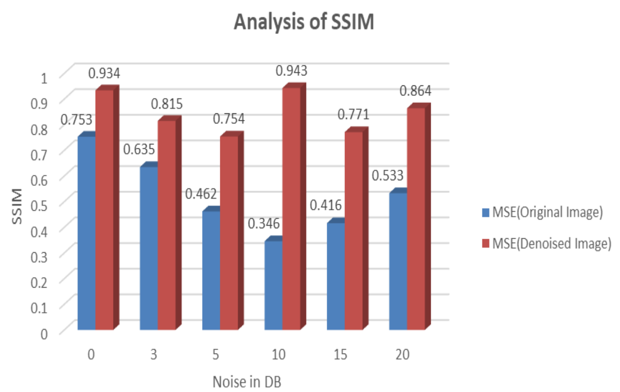

Fig. 12: Analysis of SSIM Dn-CNN.

Table 2: Analysis of PSNR, MSE, and SSIM Using CLAHE

Noise Power (dB)	PSNR	MSE	SSIM	PSNR	MSE	SSIM
	Original Image			Denoised Image		
0	52.33	0.348	0.698	53.12	0.141	0.813
3	49.56	0.298	0.721	54.16	0.215	0.747
5	45.32	0.499	0.412	51.46	0.222	0.712
10	38.56	0.898	0.423	42.53	0.543	0.844
15	41.62	0.623	0.389	51.33	0.513	0.722
20	45.23	0.321	0.498	52.26	0.142	0.821

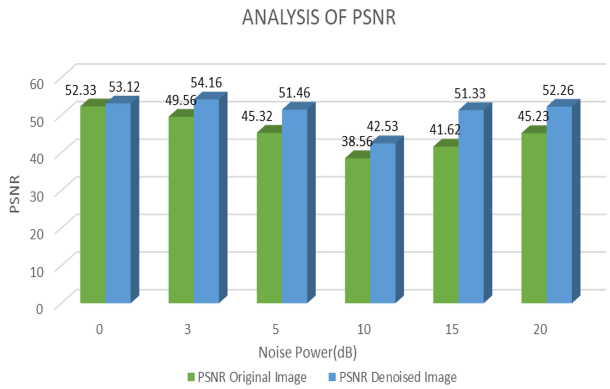

Fig. 13: Analysis of PSNR CLAHE.

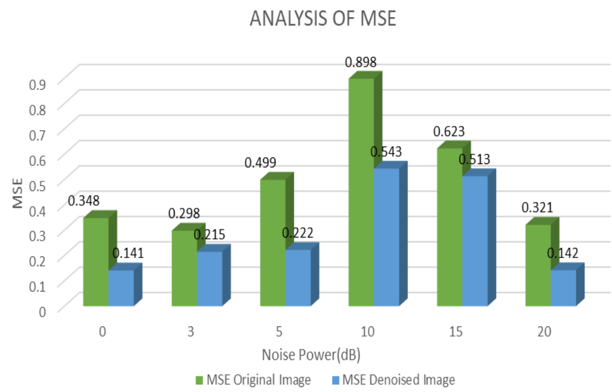

Fig. 14: Analysis of MSE Using CLAHE.

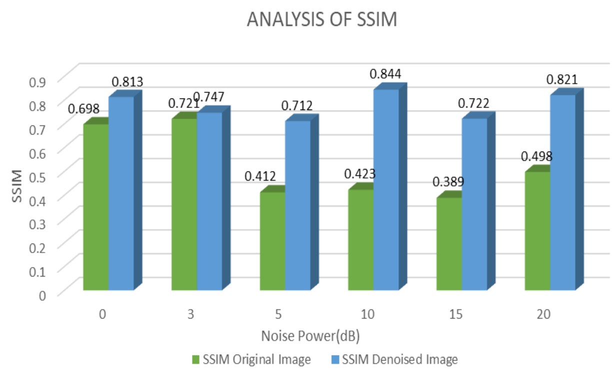

Fig. 15: Analysis of SSIM Using CLAHE.

Table 2 presents the performance of the proposed method for undersea image detection using CLAHE under various noise intensity levels. Key metrics, including MSE and PSNR, were calculated at each noise power level to assess the method's effectiveness. The proposed approach was benchmarked against an existing algorithm, with results for SSIM, PSNR, and MSE summarized in the table. Higher SSIM values reflect improved structural similarity between the processed and original images, while lower MSE and higher PSNR values indicate better image quality and reduced distortion. SSIM, in particular, serves as an indicator of perceived visual quality. Comparative results, illustrated in Figures 13, 14, and 15, further highlight the advantages of the proposed method over the existing one in terms of MSE and PSNR performance.

5. Conclusion and future enhancement

By training a Dn-CNN model on a large dataset of underwater images, aberrations can be minimized, and noise can be reduced, thereby improving the overall clarity and appeal of the images. Conversely, CLAHE (Contrast Limited Adaptive Histogram Equalization) enhances local contrast in images without excessively amplifying noise. By improving clarity and visibility, CLAHE effectively highlights the details and features of underwater images, making it easier to identify suspicious items. Together, these methods offer a comprehensive solution: CLAHE enhances local contrast and features, while Dn-CNN removes noise and restores image quality. This combined approach greatly aids in detecting objects that may have been difficult to spot in the original, degraded images. The challenges in this domain include color distortion due to the absence of natural light underwater, dynamic lighting conditions, limited visibility, and the scarcity of labeled data. However, these methods can be employed in various applications such as underwater surveillance using autonomous vehicles and robots, as well as in environmental monitoring. The proposed approach has demonstrated superior performance based on key metrics, producing higher-quality images that clearly reveal suspicious objects in underwater environments. Looking ahead, researchers could explore generative models, data augmentation techniques, and edge computing for real-time applications, further advancing the field of underwater image enhancement. Future work includes enhancing the method by integrating deep learning-based segmentation for more precise object identification. The approach can be extended to real-time underwater surveillance systems for immediate threat detection. Further optimization of DnCNN and CLAHE can be explored to improve processing speed and accuracy. Testing the model on larger and more diverse underwater datasets will ensure robustness across various environmental conditions. Finally, integrating multimodal sensor fusion techniques can enhance detection reliability in complex underwater environments. The proposed method's efficiency and robustness make it well-suited for integration into real-time systems such as autonomous underwater vehicles, enabling enhanced underwater perception and decision-making. This alignment with future advancements ensures practical deployment in dynamic and challenging underwater environments.

Conflict of interest

The authors declare that there is no conflict of interest regarding the publication of this paper.

Funding information

This research received no external funding.

Data availability

Data availability and its details are mentioned in the paper under the dataset description.

Author's contribution statement

Sangari A contributed the Literature survey and Introduction part A. Umamageswari contributed the Paper structuring and results and analysis part, S.Deepa contributed the implementation of the proposed work, and finally L.Sherin Beevi contributed the dataset collection and overall structuring of the paper.

Acknowledgement

We sincerely express our gratitude to SRM Institute of Science and Technology, Kattankulathur (SRM KTR) and the Defence Research and Development Organisation (DRDO) for providing this problem statement as part of the faculty hackathon. Their valuable contribution served as the inspiration for this work, enabling us to conceptualize and implement our ideas effectively. This support has been instrumental in shaping our research and constructing this paper.

References

[1] Ulutas, Guzin, and Beste Ustubioglu. "Underwater image enhancement using contrast-limited adaptive histogram equalization and layered difference representation." Multimedia Tools and Applications 80 (2021): 15067-15091. https://doi.org/10.1007/s11042-020-10426-2.

[2] Han, F., Yao, J., Zhu, H., & Wang, C. (2020), "Underwater image processing and object detection based on deep CNN method", Journal of Sensors, 2020. https://doi.org/10.1155/2020/6707328.

[3] Fu, X., & Cao, X. (2020). "Underwater image enhancement with global–local networks and compressed-histogram equalization", Signal Processing: Image Communication, 86, 115892https://doi.org/10.1016/j.image.2020.115892.

[4] Lee, H. S., Moon, S. W., & Eom, I. K. (2020), "Underwater image enhancement using successive color correction and superpixel dark channel prior. Symmetry", 12(8), 1220. https://doi.org/10.3390/sym12081220

[5] Alaguselvi, R., and Kalpana Murugan. "Quantitative analysis of fundus image enhancement in the detection of diabetic retinopathy using deep convolutional neural network." IETE Journal of Research (2021): 1-11. https://doi.org/10.1080/03772063.2021.1997356.

[6] S. Guo, Z. Yan, K. Zhang, W. Zuo, L. Zhang, Toward convolutional blind denoising of real photographs, in: 2019 IEEE/CVF Conference on Computer Vision and Pattern Recognition (CVPR), 2018, pp. 1712–1722, https://doi.org/10.1109/CVPR.2019.00181.

[7] C. Ledig, L. Theis, F. Huszár, J.A. Caballero, A. Aitken, A. Tejani, J. Totz, Z. Wang, W. Shi, Photo-realistic single image super-resolution using a generative adversarial network, in: 2017 IEEE Conference on Computer Vision and Pattern Recognition (CVPR), 2016, pp. 105–114, https://doi.org/10.1109/CVPR.2017.19.

[8] Sudhakara, M., & Meena, M. J. (2021), "Multi-scale fusion for underwater image enhancement using multi-layer perceptron", IAES International Journal of Artificial Intelligence, 10(2), 389. https://doi.org/10.11591/ijai.v10.i2.pp389-397.

[9] J. Chen, J. Hou, L.-P. Chau, Light field denoising via anisotropic parallax analysis in a cnn framework, IEEE Signal Process. Lett. 25 (9) (2018) 1403–1407, https://doi.org/10.1109/LSP.2018.2861212.

[10] J. Lehtinen, J. Munkberg, J. Hasselgren, S. Laine, T. Karras, M. Aittala, T. Aila, Noise2noise: Learning image restoration without clean data, 2018, arXiv preprint arXiv:1803.04189.

[11] Jian, Muwei, et al. "Underwater image processing and analysis: A review." Signal Processing: Image Communication 91 (2021): 116088. https://doi.org/10.1016/j.image.2020.116088.

[12] Singh, N., & Bhat, A. (2023). A systematic review of the methodologies for the processing and enhancement of underwater images. *Multimedia Tools and Applications*, 82, 38371–38396. https://doi.org/10.1007/s11042-023-15156-9.

[13] Hou, Guojia, et al. "An efficient nonlocal variational method with application to underwater image restoration." Neurocomputing 369 (2019): 106-121. https://doi.org/10.1016/j.neucom.2019.08.041.

[14] Muniraj, Manigandan, and Vaithiyanathan Dhandapani. "Underwater image enhancement by color correction and color constancy via Retinex for detail preserving." Computers and Electrical Engineering 100 (2022): 107909. https://doi.org/10.1016/j.compeleceng.2022.107909.

[15] Ramkumar, G., M. Ayyadurai, and C. Senthilkumar. "An effectual underwater image enhancement using deep learning algorithm." 2021 5th International Conference on Intelligent Computing and Control Systems (ICICCS). IEEE, 2021. https://doi.org/10.1109/ICICCS51141.2021.9432116.

[16] Y. Zhong, L. Liu, D. Zhao, H. Li, A generative adversarial network for image denoising, Multimedia Tools Appl. (2019) 1–13.

[17] Jiang, Qin, et al. "A novel deep neural network for noise removal from underwater image." Signal Processing: Image Communication 87 (2020): 115921. https://doi.org/10.1016/j.image.2020.115921.

[18] Lu, Huimin, et al. "Low illumination underwater light field images reconstruction using deep convolutional neural networks." Future Generation Computer Systems 82 (2018): 142-148. https://doi.org/10.1016/j.future.2018.01.001.

[19] Ding, Xueyan, et al. "Underwater image dehaze using scene depth estimation with adaptive color correction." OCEANS 2017-Aberdeen. IEEE, 2017. https://doi.org/10.1109/OCEANSE.2017.8084665.

[20] Cong, X., Zhao, Y., Gui, J., Hou, J., & Tao, D. (2024). A comprehensive survey on underwater image enhancement based on deep learning. arXiv preprint arXiv:2405.19684. https://arxiv.org/abs/2405.19684.

[21] Jamadandi, Adarsh, and Uma Mudenagudi. "Exemplar-based underwater image enhancement augmented by wavelet corrected transforms." Proceedings of the IEEE/CVF Conference on Computer Vision and Pattern Recognition Workshops. 2019.

[22] Q. Yang, P. Yan, Y. Zhang, H. Yu, Y. Shi, X. Mou, M.K. Kalra, Y. Zhang, L. Sun, G. Wang, Low-dose CT image denoising using a generative adversarial network with wasserstein distance and perceptual loss, IEEE Trans. Med. Imaging 37 (2018) 1348–1357, https://doi.org/10.1109/TMI.2018.2827462.

[23] A. Umamageswari, S. Deepa, K. Raja, "An enhanced approach for leaf disease identification and classification using deep learning techniques", Measurement: Sensors, Volume 24, 2022, 100568, ISSN2665-9174 https://doi.org/10.1016/j.measen.2022.100568.

[24] Umamageswari., Johnson, S.D., Sara, D., Kothandaraman, R. (2022). An enhanced identification andclassification algorithm for plant leaf diseases based on deep learning. Traitement du Signal, Vol. 39, No.3, pp. 1013-1018. https://doi.org/10.18280/ts.390328.

[25] K. Dabov, A. Foi, V. Katkovnik, K.O. Egiazarian, Image denoising by sparse 3-d transform-domain collaborative filtering, IEEE Trans. Image Process. 16 (2007) 2080–2095, https://doi.org/10.1109/TIP.2007.901238.

[26] K. Zhang, W. Zuo, Y. Chen, D. Meng, L. Zhang, Beyond a Gaussian denoiser: Residual learning of deep CNN for image denoising, IEEE Trans. Image Process. 26 (2017) 3142–3155, https://doi.org/10.1109/TIP.2017.2662206.

[27] P. Isola, J.-Y. Zhu, T. Zhou, A.A. Efros, Image-to-image translation with conditional adversarial networks, in: 2017 IEEE Conference on Computer Vision and Pattern Recognition (CVPR), 2016, pp. 5967–5976, https://doi.org/10.1109/CVPR.2017.632.

[28] C. Fabbri, M.J. Islam, J. Sattar, Enhancing underwater imagery using generative adversarial networks, in: 2018 IEEE International Conference on Robotics and Automation (ICRA), 2018, pp. 7159–7165, https://doi.org/10.1109/ICRA.2018.8460552.

[29] C. Li, J. Guo, C. Guo, Emerging from water: Underwater image color correction based on weakly supervised color transfer, IEEE Signal Process. Lett. 25 (2018) 323–327, https://doi.org/10.1109/LSP.2018.2792050.

[30] Y. Guo, H. Li, P. Zhuang, Underwater image enhancement using a multiscale dense generative adversarial network, IEEE J. Ocean. Eng. (2019) https://doi.org/10.1109/JOE.2019.2911447.

[31] A.Umamageswari, N.Bharathiraja, Shiny Irene (2023), "Novel fuzzy c-means based chameleon swarm algorithm for segmentation and progressive neural architecture search for plant disease classification", ICT Express – Elsevier, September 2023, Vol:9, Issue:2, pp. 160-167https://doi.org/10.1016/j.icte.2021.08.019.

[32] S. Padmapriya, A. Umamageswari, S. Deepa, and J. Faritha Banu. 2023. A novel deep learning based underwater image de-noising and detecting suspicious object. J. Intell. Fuzzy Syst. 45, 4 (2023), 7129–7144. https://doi.org/10.3233/JIFS-234002.

[33] Umamageswari, A., Deepa, S., Hussain, F.B.J., Shanmugam, P. (2024). Enhancing underwater object detection using advanced deep learning de-noising techniques. Traitement du Signal, Vol. 41, No. 5, pp. 2593-2602. https://doi.org/10.18280/ts.410532.

[34] Oleiwi, B.K., Kadhim, M.R., Real time embedded system for object detection using deep learning AIP Conference Proceedings, Volume 2415, 15 December 2022. https://doi.org/10.1063/5.0093469.

[35] Al-Tameemi, M.I., Hasan, A.A., Oleiwi, B.K.," Design and implementation monitoring robotic system based on you only look once model using deep learning technique", IAES International Journal of Artificial Intelligence, 2023, Vol. 12, No. 1, pp. 106-113. https://doi.org/10.11591/ijai.v12.i1.pp106-113.

[36] Xu, R., Zhu, D., & Chen, M. (2024). "A Novel Underwater Object Detection Enhanced Algorithm Based on YOLOv5-MH." *IET Image Processing*, vol. 18, no. 12, pp. 3415-3429. https://doi.org/10.1049/ipr2.13183.

[37] Zhou, X., Mizuno, K., & Zhang, Y. (2024). "A Self-Supervised Denoising Strategy for Underwater Acoustic Camera Imageries." *arXiv preprint arXiv:2406.02914*.

[38] Hashisho, Y., Albadawi, M., Krause, T., & von Lukas, U. (2019). "Underwater Color Restoration Using U-Net Denoising Autoencoder." *arXiv preprint arXiv:1905.09000*. https://doi.org/10.1109/ISPA.2019.8868679.

[39] Pachaiyappan, P., Chidambaram, G., Jahid, A., & Alsharif, M. H. (2024). "Enhancing Underwater Object Detection and Classification Using Advanced Imaging Techniques: A Novel Approach with Diffusion Models." *Sustainability*, vol. 16, no. 17, article 7488. https://doi.org/10.3390/su16177488.

[40] Liu, K., Sun, Q., Sun, D., Yang, M., & Wang, N. (2023). "Underwater Target Detection Based on Improved YOLOv7." *arXiv preprint arXiv:2302.06939*. https://doi.org/10.3390/jmse11030677.